ADVANCED HEALTHCARE MATERIALS
www.advhealthmat.de

Simultaneously Photo-Cleavable and Activatable Prodrug-Backboned Block Copolymer Micelles for Precise Anticancer Drug Delivery

*Dongfang Zhou, Jinshan Guo, Gloria B. Kim, Jizhen Li, Xuesi Chen, Jian Yang, and Yubin Huang**

Controlled drug release has been of great interest for decades, among which light-controllable or light-triggered drug release is of uppermost research priority due to the reason that light can offer the user-defined remote controllability as well as the temporal and spatial selectivity. To realize light-controlled drug release, endless efforts have been put on the development of photo-activatable drugs and photo-controllable drug carriers or devices.[1–3] Although frequently used as a light-controlled anti-tumor drug delivery system, small molecular photo-activatable drugs, such as photo-activated metal complexes, are quite limited by their poor water solubility, instability, short retention time, and wide distribution in healthy tissues.[4] On the other hand, photo-controllable drug carriers, especially those that are polymer-based, offer multiple advantages: they protect drugs from enzymatic or environmental cleavages and allow for high payloads and prolonged retention time.[5] More importantly, polymeric micelles can potentially demonstrate tumor targeting ability through the enhanced permeability and retention (EPR) effect or even antibody conjugation.[6]

Among polymeric photo-controllable drug carrier systems, photo-responsive block copolymer (BCP) micelles with their assembly state in aqueous solutions either controlled or changed by light have received increasing attention.[7] Many photochromic molecules have been introduced to the side chain or block junction of photo-responsive BCP micelles, including azobenzene, pyrene, spiropyran, and so on. Recently, a more attractive strategy of inserting repetitive photo-cleavable moieties, such as UV-sensitive *o*-nitrobenzyl esters into the main chains of BCPs has been developed.[8–10] These photo-cleavable group-backboned BCP micelles undergo faster photo-induced chain disintegration than the micelles with single photo-cleavable junctions between hydrophilic and hydrophobic blocks or those with multiple cleavable side groups on hydrophobic blocks. However, the above strategies often require the use of photochromic groups, which may not only increase the cytotoxicity of so-formed photo-responsive BCPs, but also release toxic byproducts after photo-treatment. Additionally, only UV light can be used as a photo-reaction trigger so the selection of light wavelengths is largely limited.[11] Furthermore, the drugs that are conjugated to the side groups or embedded in the hydrophobic cores of BCP polymers, cannot conceal the systemic toxicity of anticancer drugs due to inevitable non-specific delivery of the current nano-delivery systems.[12] All these drawbacks may present as key obstacles to the clinical application of photo-responsive BCP micelles for drug delivery.

In order to address the abovementioned challenges, the development of new chemistry and mechanism in making photo-responsive BCP micelles for more precise, controllable, tunable, effective, and safer drug delivery is urgently needed. Platinum(II) (Pt(II)) is one of the most widely used anticancer drugs and employed in 50% of all types of cancer therapy, but its application is accompanied with acquired resistance and severe toxic side effects to normal tissues.[13–15] Compared to a traditional Pt(II) drug, Pt(IV) complexes, especially photo-sensitive Pt(IV)–azide complexes, are more promising for targeted drug delivery as they are not yet activated or silenced and biocompatible under dark and can be selectively activated to release anticancer cytotoxic Pt(II) within tumor area by mild light irradiation (**Scheme 1**a).[16,17] However, most research in this area focuses on using Pt(IV)–azide complexes only as anticancer prodrugs for delivery.[18–25] We hypothesized that Pt(IV)–azide complexes could be used not only as anticancer prodrugs, but also as stimuli-responsive groups and co-monomers to construct a new class of photo-cleavable prodrug-backboned BCP micelles, as both macromolecular prodrugs and drug carriers, for mono- or multiple-drug anticancer therapy. Herein, we tested this hypothesis and developed the first simultaneously photo-cleavable and activatable (SPCA) prodrug-backboned BCP micelles using a Pt(IV)–azide complex, *trans,trans,trans*-$[Pt(N_3)_2(OH)_2(py)_2]$, which can be photo-activated by lights over a wide range of wavelengths (from UV to visible light) (Scheme 1b and Figures S1 and S2, Supporting Information). The resulting BCP micelles would have specific repeating photo-responsive prodrug units as hydrophobic blocks. In the absence of light treatment, the BCPs stayed in the silenced

Prof. D. Zhou, Prof. X. Chen, Prof. Y. Huang
State Key Laboratory of Polymer Physics and Chemistry
Changchun Institute of Applied Chemistry
Chinese Academy of Science
Changchun 130022, P. R. China
E-mail: ybhuang@ciac.ac.cn
Dr. J. Guo, Dr. G. B. Kim, Prof. J. Yang
Department of Biomedical Engineering
Materials Research Institute
The Huck Institutes of the Life Sciences
Pennsylvania State University
University Park, PA 16802, USA
Prof. J. Li
Department of Organic Chemistry
College of Chemistry
Jilin University
Changchun 130023, P. R. China

DOI: 10.1002/adhm.201600470

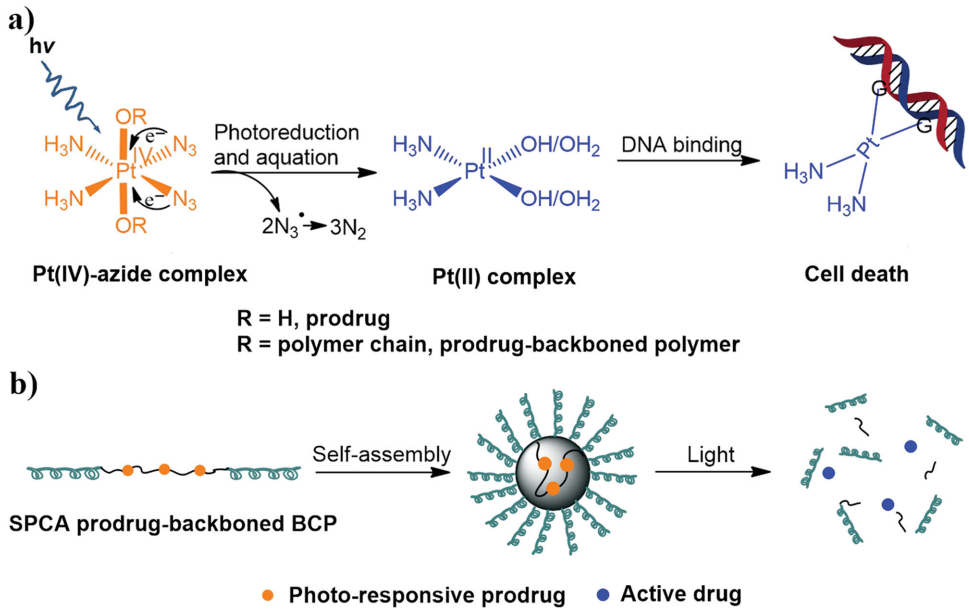

Scheme 1. Schematic illustration of a) anticancer mechanism of photo-responsive Pt(IV)–azide complexes, and b) self-assembly and light-triggered dissociation of an SPCA prodrug-backboned BCP micelle.

Pt(IV) prodrug state, which is biocompatible to normal cells. Chain cleavage and prodrug activation simultaneously occurred when light was applied, which led to the disassociation of BCP micelles and the conversion of Pt(IV) prodrug into the active Pt(II) drug, with an overall result of drug silencing without light explore and light-triggered micelle disassociation and active drug release. This strategy could conceal the systemic and local cytotoxicity of the anticancer drug against normal cells by using the silenced prodrug rather than an active anticancer drug as polymer building bricks, and circumvent the toxic side effects caused by photochromic groups and small molecular byproducts. We expect that drug release can be precisely controlled by varying the intensity and the time of light exposure, as well as the wavelength of light upon the BCP micelle system. The light triggered anticancer activity of this SPCA prodrug-backboned BCP micelle was also evaluated in vitro and in vivo.

Figure 1a shows the structure of an amphiphilic ABA triblock copolymer (PEG–PUPt(N_3)–PEG). The end block A is a water-soluble poly(ethylene glycol) (PEG) and the middle block B is a hydrophobic polyurethane with repeating photo-responsive Pt(IV)–azide prodrug bricks. The photo-cleavable PUPt(N_3) block was first prepared by step-growth polymerization of *trans,trans,trans*-[$Pt(N_3)_2(OH)_2(py)_2$] with biocompatible lysine di-isocyanate (LDI), which was slightly in excess to preserve terminated isocyanate (NCO) groups. The bi-isocyanate terminated PUPt(N_3) (NCO–PUPt(N_3)–NCO) was then reacted with monomethyl ether PEG_{2k} (2000 g mol^{-1}) to yield the triblock copolymer PEG–PUPt(N_3)–PEG (Scheme S2, Supporting Information). The successful coupling of PUPt(N_3) and PEG was confirmed by the molecular weight (M_n) of PEG–PUPt(N_3)–PEG (7800 g mol^{-1}) determined by gel permeation chromatography (GPC) (Figure 1b), which is in agreement with the ^{1}H-NMR result (Figure S3, Supporting Information). The M_n of PUPt(N_3) block was calculated to be 3800 g mol^{-1} and the polymerization degree was roughly estimated to be 5. The platinum content determined by inductively coupled plasma optical emission spectroscopy (ICP-OES) was 13 wt%, with a drug loading of ≈23 wt% prodrug in each BCP chain, which is higher than that of previously reported polymer–drug conjugate systems.[26,27] Stable aggregates can be formed after dissolving PEG–PUPt(N_3)–PEG in THF and dialyzing against water (Figure S5, Supporting Information). Because Pt is a heavy metal, the TEM images could be visualized without normal staining. The transmission electron microscopy (TEM) image shows that PEG–PUPt(N_3)–PEG formed clear spherical core–shell BCP micelles with a narrow size distribution (Polydispersity index = 0.108) and a low critical micelle concentration (CMC = 4.66×10^{-3} g L^{-1}) (**Figure 2**b and Figure S6, Supporting Information). The average hydrodynamic diameter of the micelles determined by dynamic light scattering (DLS) was ≈ 144 nm (Figure 2a).

Photo-induced cleavage of PEG–PUPt(N_3)–PEG polymer chains in THF solution and dissociation of these BCP micelles in aqueous solutions were both investigated. The molecular weight change of BCP before and after light irradiation, obtained by GPC, is shown in Figure 1b. Without irradiation, the M_n of PEG–PUPt(N_3)–PEG kept unchanged in THF over one week. After irradiation of BCP solution with light (365 nm, 10 mW cm^{-2}) for 60 min, the GPC curve showed a dominant group of low-molecular-weight species while a remaining polymer peak matched the elution peak of PEG_{2k}. This implies a complete scission of PEG chains from PUPt(N_3) as well as the severe disintegration of the hydrophobic PUPt(N_3) block into low-molecular-weight species. X-ray photoelectron spectroscopy (XPS) was used to identify the oxidation state of Pt in the BCP and the low-molecular-weight species after irradiation (Figure 1c). Pt_{4f} in PEG–PUPt(N_3)–PEG (77.9 and 74.6 eV) exhibited the characteristic binding energies of Pt(IV) close to those of Pt(IV)–azide prodrug (78.5 and 75.3 eV). While, the binding energies for Pt_{4f} in the low-molecular-weight species

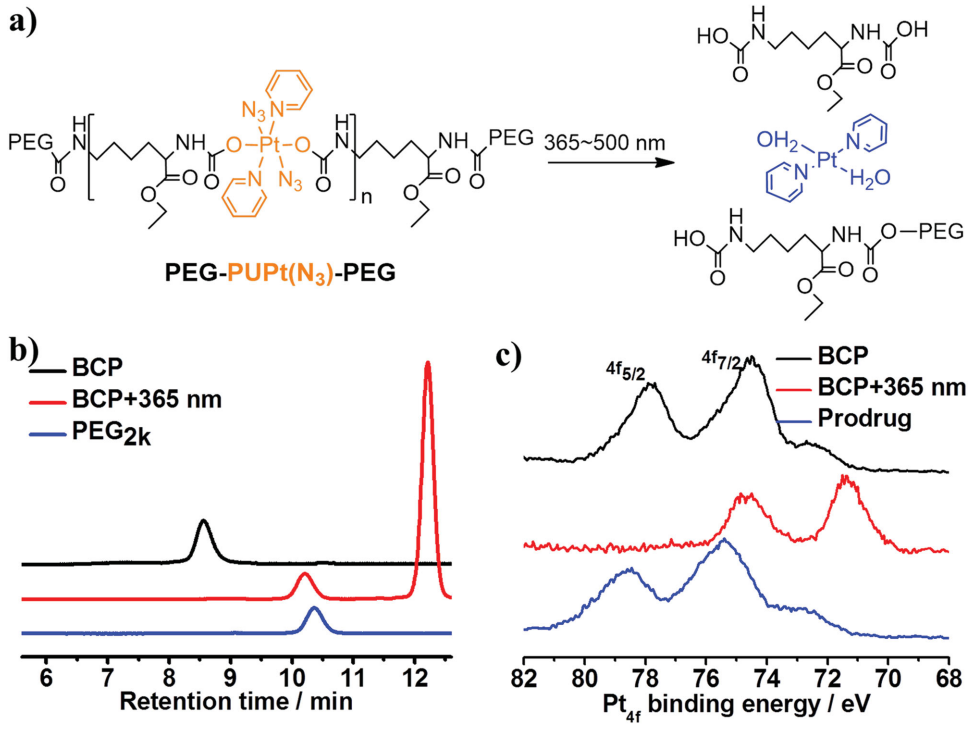

Figure 1. a) Light-triggered chain cleavage of the SPCA prodrug-backboned BCP, PEG–PUPt(N_3)–PEG, b) GPC curves of PEG_{2k}, PEG–PUPt(N_3)–PEG before and after 365 nm light irradiation (10 mW cm^{-2}, 60 min), and c) XPS curves of Pt_{4f} in prodrug, PEG–PUPt(N_3)–PEG before and after 365 nm light irradiation (10 mW cm^{-2}, 60 min).

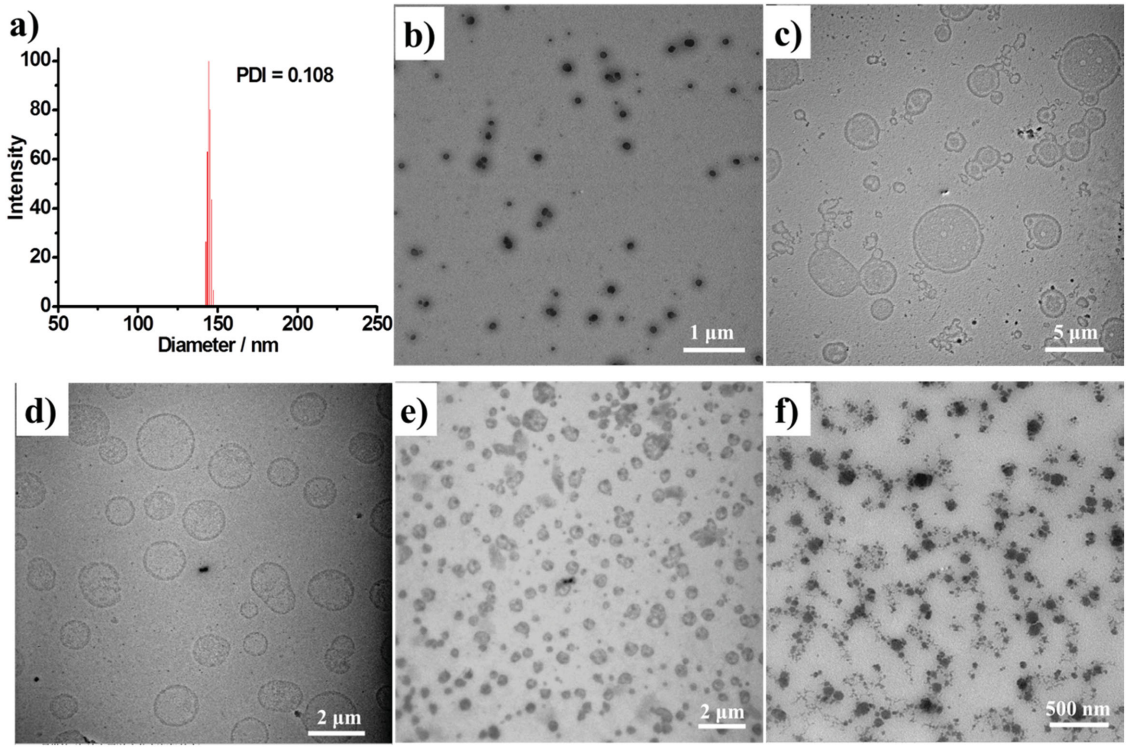

Figure 2. a) DLS characterization and b) TEM image of the SPCA prodrug-backboned BCP micelles in the dark, and TEM images of micelles after light irradiation (10 mW cm^{-2}) applied for 60 min at: c) 365, d) 400, e) 430, and f) 500 nm.

were 73.7 and 71.2 eV, indicating the activation of Pt(IV)–azide prodrug in BCP to active Pt(II) complex upon irradiation (Figure 1a).[28,29] The simultaneously occurred rapid photo-activation of Pt(IV) to Pt(II) and photo-cleavage of the PUPt(N_3) block can lead to disintegration of the BCP micelle in aqueous solutions too (Figure S7, Supporting Information). According to previous conclusion that *trans,trans,trans*-[$Pt(N_3)_2(OH)_2(py)_2$] could be photo-activated by UV to green lights,[30] we monitored the micelle disintegration process under light irradiation within a range of wavelengths (365, 400, 430, and 500 nm, 10 mW cm^{-2}) using TEM and DLS (Figure 2c–f and Figure S8, Supporting Information). After light exposure for 1 h, the complete disintegration of micelles' hydrophobic cores into vesicles was observed at all wavelengths except 500 nm. The fusion process of these vesicles into much larger capsules was also observed, agreeing with the DLS results (Figures S9–S12, Supporting Information). These results indicate that light with a wide range of wavelengths can trigger the cleavage/dissociation of PEG–PUPt(N_3)–PEG polymer chains/micelles.

To further study the wavelength-regulated photo-responsive behavior of PEG–PUPt(N_3)–PEG micelles, we recorded the change of their UV–vis spectra under light irradiation at the four different wavelengths mentioned above. As shown in **Figure 3**a, PEG–PUPt(N_3)–PEG micelles possess ligand to metal charge-transfer (LMCT) UV–vis absorbance centered at 298 nm, the same as Pt—N_3 in free prodrug (Figure S13, Supporting Information). Micelles showed a rapid response to all irradiations (Figure S14, Supporting Information). The UV–vis peak at 298 nm drastically decreased after light irradiation, indicating the rapid cleavage of Pt—N_3 bond and simultaneous reduction of Pt(IV) to Pt(II).[30–32] By plotting normalized absorbance at 298 nm versus irradiation time, we found that the absorbance of micelles dropped a little more rapidly than the original small prodrug upon light irradiation (Figure 3b). It demonstrated that copolymerization of a strong electron withdrawing monomer LDI with *trans,trans,trans*-[$Pt(N_3)_2(OH)_2(py)_2$] did not affect the photo-activation of the prodrug but even made this process faster. The photo-reduction of BCP micelles almost followed first order kinetics under 430 nm radiation, and the photo-reduction rates were in the order of 365 > 400 > 430 > 500 nm (Figure 3b). Fast degradation of PEG–PUPt(N_3)–PEG micelles backbone should only occur when the Pt(IV)–azide prodrug was photo-reduced to active Pt(II). Once the light irradiation is stopped, the photo-reduction should stop as well, resulting in a pause in backbone degradation. The degradation should not resume until the light trigger is reapplied. To prove our hypothesis, the absorbance of PEG–PUPt(N_3)–PEG micelles in response to periodic light irradiation at 298 nm was monitored. As expected, when irradiation was turned on for 10 min and then off for 50 min, pulsatile drops of the absorbance of the micelles were observed at 298 nm during the 10 min light-on periods, and the absorbance remained constant during the 50 min light-off periods (Figure 3c).

The potential to release anticancer drugs on-demand and release profiles from PEG–PUPt(N_3)–PEG micelles were also investigated. The release of Pt(II) from micelles was detected by ICP-OES in water. Without irradiation, the proportion of Pt released from the micelles in water was nearly negligible

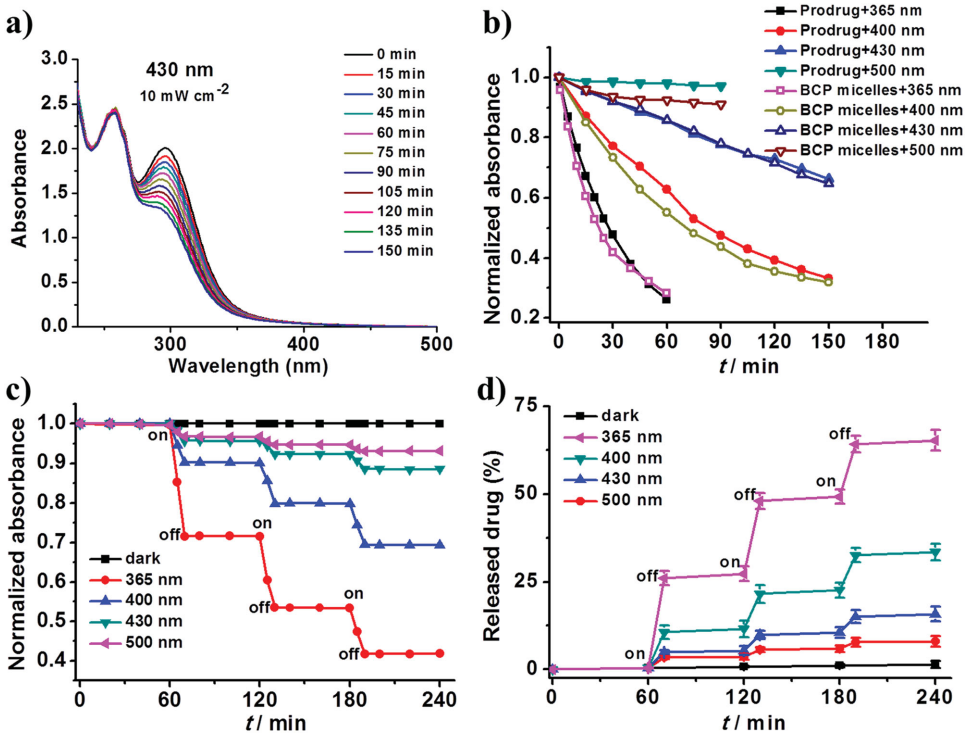

Figure 3. a) UV–vis spectra of SPCA prodrug-backboned BCP micelles upon irradiation (430 nm, 10 mW cm^{-2}) for the indicated periods of time (0–150 min), b) normalized UV absorption of prodrug and BCP micelles at 298 nm drop over time, c) normalized UV absorption of BCP micelles at 298 nm of micelles under light off and on in an intermittent manner, and d) platinum release profiles of BCP micelles detected by ICP-OES in water in the presence of intermittent light irradiation.

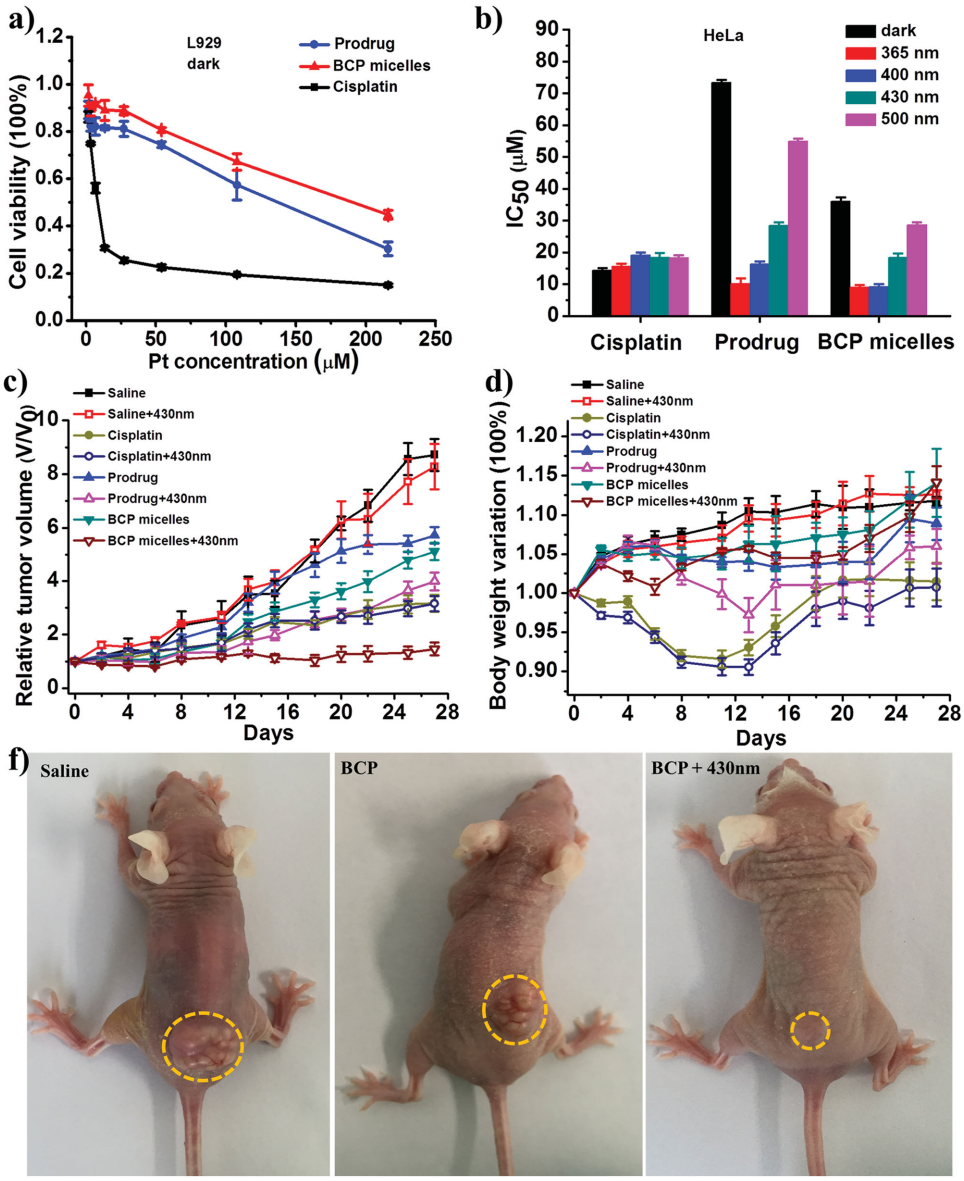

Figure 4. a) In vitro cytotoxicity curves of cisplatin, prodrug, and SPCA prodrug-backboned BCP micelles against L929 normal fibroblasts in the dark, b) IC_{50} values of cisplatin, prodrug, and SPCA prodrug-backboned BCP micelles against HeLa cancer cell in the dark and in the presence of 365, 400, 430, and 500 nm light irradiation during 48 h incubation, c) tumor growth inhibition curves, and d) body weight variation profiles of female BALB/c nude mice bearing A549 xenografts at the back after intravenous injection of saline, cisplatin (3 mg kg^{-1}), prodrug (2 mg Pt kg^{-1}), and SPCA prodrug-backboned BCP micelles (2 mg Pt kg^{-1}), and e) photo images of mice (orange circle, xenografts) on day 27 after intravenous injection of saline and SPCA prodrug-backboned BCP micelles (without and with light irradiation). Data are expressed as mean ± standard deviation, $n = 5$, $^*P < 0.05$.

(Figure 3d). Pulsatile release of Pt(II) from the micelles was observed with periodic light irradiation at all enabled wavelengths, corresponding to the above "on-off" drops of the absorbance at 298 nm of the micelles. After three "on-off" cycles, 65.3% of the reduced Pt(II) was released at 365 nm, 33.5% at 400 nm, 15.7% at 430 nm, and 8% at 500 nm. All these results demonstrated that PEG–PUPt(N_3)–PEG micelles display excellent "on-off" controllable photo-responsiveness to a wide range of wavelengths (from UV to visible light). These properties could be beneficial for remote control over Pt drug release at different depths within tumor tissues as well as release rates and release modes.

The cell cytotoxicity against normal cells and cancer cells of the SPCA prodrug-backboned BCP under dark and after light irradiation was assessed by methyl thiazolyl tetrazolium (MTT) assay using cisplatin and small prodrug as control (Table S1, Supporting Information). Cell viability reached over 98% after irradiation at varied wavelengths in the absence of any drug (Figure S15, Supporting Information). Without light treatment, cisplatin still killed both HeLa cervical cancer cells and L929 normal fibroblasts without selectivity (**Figure 4** and Figures S16 and S17, Supporting Information). While, PEG–PUPt(N_3)–PEG micelles exhibited much lower cytotoxicity than that of cisplatin and even small prodrug against normal cells,

indicating toxic side effect remission ability of the micelles against normal cells. Upon light treatment, all IC_{50} values (50% inhibiting concentration) for the small prodrug and BCP micelles against cancer cells decreased dramatically as anticipated (Figure 4b), since the Pt(IV)–azide complexes were reduced to the more toxic Pt(II) form after light irradiation. PEG–PUPt(N_3)–PEG micelles were found to be roughly 1.5–4-fold more cytotoxic against HeLa cells upon light irradiation than in the dark, suggesting that the cytotoxicity of micelles can be effectively controlled by external light stimulations. This is in agreement with the photosensitivity results shown in Figure 3. Micelles also showed much higher cytotoxicity than that of equal-dose small prodrug under all wavelengths. Micelles activated by 365 and 400 nm lights were twofold effective than cisplatin. Even visible light (430 and 500 nm) activated micelles exhibited comparable efficacy with cisplatin, the most widely clinically used Pt drug. Similar results were also observed in A549 lung cancer cells (Figure S17, Supporting Information). These results demonstrated that our established SPCA prodrug-backboned BCP micelles, as platinum-based drug delivery devices, can be light-activated at the tumor site to selectively kill cancer cells, and the anticancer cytotoxicity could also be well-regulated by controlling intensity, duration, and wavelengths of irradiation light.

Finally, we evaluated the light-triggered therapeutic efficacy of the SPCA prodrug-backboned BCP micelles in vivo against subcutaneous A549 tumors developed by tumor cells injected in the back of BALB/c nude mice. Cisplatin (3 mg kg^{-1}), prodrug (2 mg Pt kg^{-1}), and PEG–PUPt(N_3)–PEG micelles (2 mg Pt kg^{-1}) were administered intravenously for three times on day 0, day 3, and day 7 under dark. Mice were then split into two groups: one group was kept constantly under dark and the other group was irradiated with green light (430 nm, 10 mW cm^{-2}, deep tumor penetrative and harmless) at the tumor site for 1 h on day 1, day 4, and day 8. After light treatment, mice were placed back to the dark. Tumor growth inhibition effects in the presence and absence of light treatment are shown in Figure 4c. The prodrug was only slightly more effective in inhibiting tumor growth upon light irradiation than under dark, likely due to the rapid blood clearance of small molecular drugs by the kidney. The anti-tumor effect of PEG–PUPt(N_3)–PEG micelles was greatly enhanced upon light irradiation, implying the greatest efficacy when compared to the prodrug and even cisplatin, in agreement with the cytotoxicity results in vitro. Tumor growth was completely suppressed without excessive growth even over four weeks (Figure 4e). The change of body weight was also monitored to determine systemic toxicity (Figure 4d). Administration of cisplatin both under dark and after light irradiation led to a significant decrease in the total body weight during the first two weeks. Under dark, both prodrug and SPCA prodrug-backboned BCP micelles showed less effect on weight gain of mice compared with cisplatin. After light treatment, the systemic toxicity of the prodrug appeared on day 8, while PEG–PUPt(N_3)–PEG micelles only caused a slight effect on the body weight. These results demonstrate that PEG–PUPt(N_3)–PEG micelles were able to enhance anti-tumor efficacy while decrease systemic toxicity in vivo.

It is important to note that polymeric drug delivery vehicles have the ability to improve drug pharmacokinetics, biodistribution, and tissue-specific accumulation, resulting in enhanced

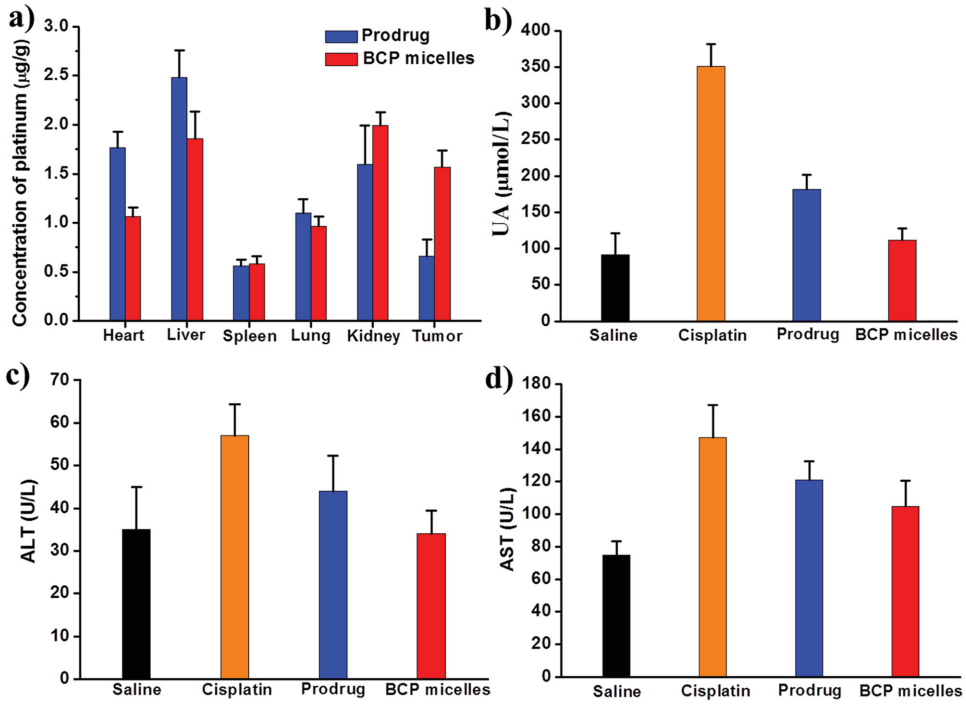

Figure 5. a) Biodistribution of platinum for prodrug and SPCA prodrug-backboned BCP micelles after 24 h single intravenous administration at a 2 mg Pt kg^{-1} in KM mice; b) UA, c) ALT, d) AST levels alteration at one week after intravenous administration of saline, cisplatin (3 mg kg^{-1}), prodrug (2 mg Pt kg^{-1}), and SPCA prodrug-backboned BCP micelles (2 mg Pt kg^{-1}).

efficacy and improved tolerability.[33] Indeed, biodistribution study showed that SPCA prodrug-backboned BCP micelles achieved a significant higher Pt concentration (twofold) in tumor tissue than that of free prodrug after administration for 24 h through the EPR effect (**Figure 5**a). We also found that the concentrations of Pt in all tissues except kidney following administration of the BCP micelles were lower than what was attained following administration of free prodrug. The higher levels of blood biochemistry parameters aspartate aminotransferase (AST) and alanine aminotransferase (ALT) associated with the function of liver and uric acid (UA) associated with the function of kidney resulting from cisplatin and prodrug treated mice than control group indicated the severe hepatotoxicity and renal toxicity induced by free small drugs. All the data presented herein suggest that the BCP micelles may effectively alleviate nephrotoxicity and neurotoxicity (Figure 5b–d). These results demonstrate that cisplatin exhibited high systemic toxicity while PEG–PUPt(N_3)–PEG micelles could reduce the side effects and improve the total life quality of mice undergoing chemotherapy.

In conclusion, for the first time, a novel SPCA prodrug-backboned BCP micelle strategy for anticancer drug delivery was developed by utilizing Pt(IV)–azide complexes not only as anticancer prodrugs, but also as co-monomers and stimuli-responsive groups. Tunable and pulsatile active Pt(II) drug release upon applied light triggers at a wide range of wavelengths (from UV to visible light) from the BCPs was realized. The excellent photo-responsive cytotoxicity and in vivo antitumor efficacy and toxic side effect remission ability of the BCP micelles were also demonstrated by applying external temporal and spatial controlled stimulations. The photo-cleavability and photo-activatability render this class of SPCA prodrug-backboned BCP micelles with both light-responsibility and cell selectivity, benefited from both the temporal and spatial selectivity of light trigger and the application of more biocompatible prodrug rather than active anticancer drugs. It may also become important building blocks for preparing the next-generation controlled release devices and personalized nano-medicine for in vivo applications. Finally, it can also be reasonably anticipated that, the unique SPCA prodrug-backboned BCP mechanism can be used as a drug carrier to load other anticancer drugs and can help to fabricate multidrug systems for combination therapy.

Supporting Information

Supporting Information is available from the Wiley Online Library or from the author.

Acknowledgements

The authors would like to thank the financial support from the National Natural Science Foundation of China (Nos. 51403198 and 51573069) and Jilin Provincial Science and Technology Department (No. 20150520019JH). All animal experiments were approved by the local institution review board and performed according to the Guidelines of the Committee on Animal Use and Care of Changchun Institute of Applied Chemistry, Chinese Academy of Sciences.

Received: April 27, 2016
Revised: June 20, 2016
Published online: July 27, 2016

[1] B. P. Timko, T. Dvir, D. S. Kohane, *Adv. Mater.* **2010**, *22*, 4925.
[2] C. Bao, L. Zhu, Q. Lin, H. Tian, *Adv. Mater.* **2015**, *27*, 1647.
[3] M. A. Shaker, H. M. Younes, *J. Controlled Release* **2015**, *217*, 10.
[4] P. J. Bednarski, F. S. Mackay, P. J. Sadler, *Anti-Cancer Agents Med. Chem.* **2007**, *7*, 75.
[5] A. Y. Rwei, W. Wang, D. S. Kohane, *Nano Today* **2015**, *10*, 451.
[6] H. Wei, R. Zhuo, X. Zhang, *Prog. Polym. Sci.* **2013**, *38*, 503.
[7] Y. Zhao, *Macromolecules* **2012**, *45*, 3647.
[8] D. Han, X. Tong, Y. Zhao, *Macromolecules* **2011**, *44*, 437.
[9] D. Han, X. Tong, Y. Zhao, *Langmuir* **2012**, *28*, 2327.
[10] Y. Zhang, Q. Yin, L. Yin, L. Ma, L. Tang, J. Cheng, *Angew. Chem. Int. Ed.* **2013**, *52*, 6435.
[11] A. Barhoumi, Q. Liu, D. S. Kohane, *J. Controlled Release* **2015**, *219*, 31.
[12] J. F. Gohy, Y. Zhao, *Chem. Soc. Rev.* **2013**, *42*, 7117.
[13] L. Kelland, *Nat. Rev. Cancer* **2007**, *7*, 573.
[14] J. J. Wilson, S. J. Lippard, *Chem. Rev.* **2014**, *114*, 4470.
[15] H. Lian, M. Hu, C. Liu, Y. Yamauchi, K. C. Wu, *Chem. Commun.* **2012**, *48*, 5151.
[16] N. Graf, S. J. Lippard, *Adv. Drug Delivery Rev.* **2012**, *64*, 993.
[17] J. S Butler, P. J. Sadler, *Curr. Opin. Chem. Biol.* **2013**, *17*, 175.
[18] Y. Dai, H. Xiao, J. Liu, Q. Yuan, P. Ma, D. Yang, C. Li, Z. Cheng, Z. Hou, P. Yang, J. Lin, *J. Am. Chem. Soc.* **2013**, *135*, 18920.
[19] Y. Min, J. Li, F. Liu, E. K. Yeow, B. Xing, *Angew. Chem. Int. Ed.* **2014**, *53*, 1012.
[20] H. Xiao, G. T. Noble, J. F. Stefanick, R. Qi, T. Kiziltepe, X. Jing, B. Bilgicer, *J. Controlled Release* **2014**, *173*, 11.
[21] H. Song, W. Li, R. Qi, L. Yan, X. Jing, M. Zheng, H. Xiao, *Chem. Commun.* **2015**, *51*, 11493.
[22] D. Zhou, S. He, Y. Cong, Z. Xie, X. Chen, X. Jing, Y. Huang, *J. Mater. Chem. B* **2015**, *3*, 4913.
[23] A. Gandioso, E. Shaili, A. Massaguer, G. Artigas, A. G. Canto, J. A. Woods, P. J. Sadler, V. Marchan, *Chem. Commun.* **2015**, *51*, 9169.
[24] H. Song, X. Kang, J. Sun, X. Jing, Z. Wang, L. Yan, R. Qi, M. Zheng, *Chem. Commun.* **2015**, *51*, 11493.
[25] S. He, Y. Qi, G. Kuang, D. Zhou, J. Li, Z. Xie, X. Chen, X. Jing, Y. Huang, *Biomacromolecules* **2016**, *17*, 2120.
[26] H. Xiao, R. Qi, S. Liu, X. Hu, T. Duan, Y. Zheng, Y. Huang, X. Jing, *Biomaterials* **2011**, *32*, 7732.
[27] D. Zhou, H. Xiao, F. Meng, X. Li, Y. Li, X. Jing, Y. Huang, *Adv. Healthcare Mater.* **2013**, *2*, 822.
[28] X. Gang, H. Zhu, Y. Shi, W. Tang, *Biometals* **2001**, *14*, 51.
[29] H. Xiao, D. Zhou, S. Liu, Y. Zheng, Y. Huang, X. Jing, *Acta Biomater.* **2012**, *8*, 1859.
[30] N. J. Farrer, J. A. Woods, L. Salassa, Y. Zhao, K. S. Robinson, G. Clarkson, F. S. Mackay, P. J. Sadler, *Angew. Chem., Int. Ed.* **2010**, *49*, 8905.
[31] J. S. Butler, J. A. Woods, N. J. Farrer, M. E. Newton, P. J. Sadler, *J. Am. Chem. Soc.* **2012**, *134*, 16508.
[32] F. S. Mackay, J. A. Woods, P. Heringova, J. Kasparkova, A. M. Pizarro, S. A. Moggach, S. Parsons, V. Brabec, P. J. Sadler, *Proc. Natl. Acad. Sci. USA* **2007**, *104*, 20743.
[33] S. Dhar, N. Kolishetti, S. J. Lippard, O. C. Farokhzad, *Proc. Natl. Acad. Sci. USA* **2011**, *108*, 1850.

